Journal of Advanced Research (2012) 3, 167–175

Cairo University

Journal of Advanced Research

ORIGINAL ARTICLE

Effect of different additions on the crystallization behavior and magnetic properties of magnetic glass–ceramic in the system Fe_2O_3–ZnO–CaO–SiO_2

Salwa A.M. Abdel-Hameed [a,*], **Abeer M. El Kady** [b]

[a] *Glass Research Department, National Research Center, Dokki, ElBehoos St., Cairo 126222, Egypt*
[b] *Biomaterial Department, National Research Center, Dokki, ElBehoos St., Cairo 126222, Egypt*

Received 13 April 2011; revised 3 July 2011; accepted 3 July 2011
Available online 10 August 2011

KEYWORDS

Magnetite nanocrystals;
Glass–ceramic;
Ferrimagnetic;
Hyperthermia;
Cancer

Abstract This work pointed out the preparation of a magnetic glass–ceramic in the system Fe_2O_3·ZnO·CaO·SiO_2. The base composition was designed to crystallize about 60% magnetite. The influence of adding TiO_2, Na_2O and P_2O_5 separately or as mixtures was studied. The DTA of the glasses revealed a decrease in the thermal effects by adding P_2O_5, TiO_2 and Na_2O in an increasing order. The X-ray diffraction patterns showed the presence of nanometric magnetite crystals in a glassy matrix after cooling from the melting temperature. The crystallization of magnetite increased by adding TiO_2, and P_2O_5, respectively, and decreased by adding Na_2O. Heat treatment was carried out for the glasses in the temperature range of 1000–1050 °C, for different time periods, and led to the appearance of hematite and β-wollastonite, which was slightly increased by adding P_2O_5 or TiO_2 and greatly enhanced by adding Na_2O. Samples containing mixtures of TiO_2, Na_2O, and P_2O_5 showed a summation of the effects of those oxides. The microstructure of the samples was examined by using TEM, which revealed a crystallite size of magnetite to be in the range of 52–90 nm. Magnetic hysteresis cycles were analyzed using a vibrating sample magnetometer with a maximum applied field of 10 kOe at room temperature in quasi-static conditions. From the obtained hysteresis loops, the saturation magnetization (M_s), remanence magnetization (M_r) and coercivity (H_c) were determined. The results showed that the prepared magnetic glass–ceramics are expected to be useful for a localized treatment of cancer.

* Corresponding author. Tel.: +20 2 33371362x1325; fax: +20 2 33387803.
E-mail address: Salwa_NRC@hotmail.com (S.A.M. Abdel-Hameed).

Peer review under responsibility of Cairo University.
doi:10.1016/j.jare.2011.07.001

Production and hosting by Elsevier

Introduction

Nanoparticles ferrimagnetic glass–ceramics seem to play an essential role in the future technology, especially in different health care uses, such as cell separation, magnetic resonance imaging contrast agents, drug delivery and hyperthermia treatment of cancer [1–4].

Hyperthermia destroys cancer cells, by raising the tumor temperature to a "high fever" range, similar to the way that the body naturally does to combat other forms of diseases

[3]. Generally, tumors are more easily heated than the surrounding normal tissues. Blood vessels and nervous systems are poorly developed in the tumor mass. Therefore, oxygen supply that reaches the tumor via those vessels is not sufficient, which leads to the death of cancer cells by heat treatment. Hence hyperthermia is expected to be very useful in cancer treatment. Moreover, hyperthermia has no side effects on the healthy tissue that surround the tumor and has efficient blood cooling systems [4,5].

The importance of magnetic nanoparticles or nanocrystals comes from their remarkable new phenomena, such as superparamagnetism, high field irreversibility, high saturation field, and extra anisotropy contributions or shifted loops after field cooling. These phenomena arise from the finite size and surface effects that dominate the magnetic behavior of individual nanoparticles or nanocrystals [1,6,7].

In a previous work we have designed to precipitate ~60% nanocrystals of magnetite in two different compositions based on the crystallization of hardystonite ($Ca_2ZnSi_2O_7$), or wollastonite ($CaSiO_3$), beside magnetite [4] and we have found that, crystallization of magnetite nanocrystals was enhanced greatly in the presence of Zn ions and consequently the saturation magnetization was enhanced and reached the value of 52.13 emu/g.

In the presented work, we have tried to improve the previously obtained magnetic properties [4]. This was carried out through the investigation of the influence of the addition of different oxides, such as TiO_2, Na_2O and P_2O_5, on the amount and grain size of the precipitated magnetite nanocrystals in the system $Fe_2O_3{\cdot}CaO{\cdot}ZnO{\cdot}SiO_2$. These oxides were chosen because they were known to cause a decrease in the viscosity of the melt, enhancing the phase separation process and consequently enhancing the crystallization process [8–14].

Material and methods

Preparation of glasses

The glass was designed to crystallize ~60% magnetite and 40% hardystonite. The study of the effect of adding TiO_2, Na_2O and P_2O_5 separately or as mixtures on the crystallization sequence, and magnetic properties, was carried out. The samples were denoted as FHP, FHN, FHT and FHPNT according to the oxide additions. The chemical compositions of the examined glasses as well as their codes are shown in Table 1. About 100 g powder mixtures of these compositions were prepared from the reagent grade of CaO (as Ca_2CO_3), SiO_2, Fe_2O_3, and ZnO. In addition, B_2O_3 (as H_3BO_3), TiO_2, Na_2O (as Na_2CO_3) and P_2O_5 (as $NH_4H_2PO_4$) were added above 100%. Our target was to obtain glass–ceramics, not ceramic materials, so a melting step was necessary to achieve the nucleation of magnetite in a liquid-derived amorphous phase. The batches were placed in a platinum crucible, and melted in an electric furnace, at 1350 °C for 2 h. The melts were poured onto a stainless steel plate, at room temperature, and pressed into a plate of 1–2 mm thick by another cold steel plate.

Crystallization of glasses

Thermal behavior of our samples was examined using differential thermal analysis (DTA). DTA was performed using SETRAM Instrumentation Regulation, Labsys™ TG-DSC16 under inert gas. According to the DTA results, the obtained glasses were subjected to different heat treatment schedules. This was carried out to study the effect of applying different temperatures on their crystallization behavior. Samples plates were covered with active carbon powder during the heat treatment, to apply a reducing atmosphere, and to prevent the ferrous ions from oxidizing while heating up the samples, at a rate of 3 °C/min, up to various crystallization temperatures. Heating of samples was carried out in a SiC electric furnace. It was noticed that the synthesis parameters (such as temperature, time, heating rate, and atmosphere) play a fundamental role for magnetite crystallization.

Characterization

The heat treated glasses were subjected to powder X-ray diffraction analysis (XRD), using Ni-filled Cu-Kα radiation, to determine the types and contents of the crystalline phases precipitated as a result of their crystallization. XRD was performed using Pruker D8 Advanced instrument. The average crystallite size of magnetite, precipitated in the as prepared glasses, and of those subjected to heat treatment, was determined for its most intense peaks (220, 311, 400, 511 and 440), from their XRD patterns, by using Debye–Scherrer formula:

$$D = k\lambda / B\cos\Theta$$

where D is the particle size, k is constant, λ for Cu is 1.54 Å, B is the full half wide and $2\Theta = 4°$. The heat treated glasses were crushed, and sonically suspended in ethanol. Few drops of the suspended solution were placed on an amorphous carbon film held by copper microgrid mesh and were observed under transmission electron microscope (ZEISS Germany).

The magnetic properties of the as prepared and heat treated samples were measured at room temperature using a vibrating sample magnetometer (VSM; 9600-1 LDJ, USA) in a maximum applied field of 10 kOe. From the obtained hysteresis loops, the saturation magnetization (M_s), remanence magnetization (M_r) and coercivity (H_c) were determined.

Table 1 Chemical composition of the studied glasses in wt.%.[a]

Sample	Fe_2O_3	CaO	ZnO	SiO_2	B_2O_3	P_2O_5	Na_2O	TiO_2
FH	60	14.3	10.38	15.32	3	–	–	–
FHP	60	14.3	10.38	15.32	3	3	–	–
FHN	60	14.3	10.38	15.32	3	–	3	–
FHT	60	14.3	10.38	15.32	3	–	–	3
FHPNT	60	14.3	10.38	15.32	3	3	3	3

[a] B_2O_3, P_2O_5, Na_2O and TiO_2 were added above 100%.

Results and discussion

The compositions of all glasses were not significantly different. Therefore, the observed thermo-physical properties of all the glasses were similar with respect to their T_g, T_c, and μH values. However, it was clear that any slight changes in their composition, by the introduction of nucleating agents, may have dramatic effects on the chronology and morphology of the precipitated phases [15]. Fig. 1 and Table 2 reveal the thermal behavior of the samples under investigation. All the samples showed transformation temperatures in the range of 587–662 °C, and one exothermic peak in the range of 788–840 °C. It could be noticed that the temperatures of the thermal effects increased by adding P_2O_5 (FHP) than that of the base glass (FH), while the addition of Na_2O led to a significant decrease in all the temperatures of the thermal effects. The addition of TiO_2 (FHT) showed thermal effects similar to that of the base glass. The addition of mixtures of P_2O_5, TiO_2 and Na_2O (FHPNT) led to slight shifts in T_g and exothermic peaks to lower temperatures. This effect was due to the summation of the individual oxide effects. It should be noted that the increase in all the exothermic and endothermic peaks indicates an increase in the amount of magnetite phase precipitated in the quenched glass and led to observed thermal transformation processes that occurred at higher temperatures, and the opposite is right [2]. Furthermore, the peaks of FHN had larger areas and, consequently, had higher enthalpy than those recorded for FHT, FHPNT and FHP, respectively. This can be attributed to the fact that the addition of P_2O_5 greatly enhances the precipitation of the magnetite in glass melts during their cooling from the melting temperatures, while the addition of Na_2O had a significant effect on inhibiting magnetite formation during cooling. On the other hand, the addition of TiO_2 had increased the amount of crystallized magnetite; however, its effect was slightly lower than that caused by the addition of P_2O_5. All curves showed a glass transition temperature (T_g) typical of an amorphous phase. The T_g values of glass–ceramics are useful as an indicator of the amount of SiO_2 in the residual glass [11]. The presence of the glass transition temperature confirmed the presence of a reasonable amount of residual amorphous phases in all the glass–ceramic samples. As the amount of magnetite in the quenched glass was increased, the T_g was increased. The glass transition temperatures of the prepared glass–ceramics were similar to those of

Table 2 DSC results of samples under investigation.

Sample	T_g (°C)	Exothermic peak (°C)	Enthalpy (μV s/mg)
FH	662	838	−10.4299
FHP	683	840	−3.7129
FHN	587	788	−15.3775
FHT	662	831	−12.0901
FHPNT	639	830	−11.3595

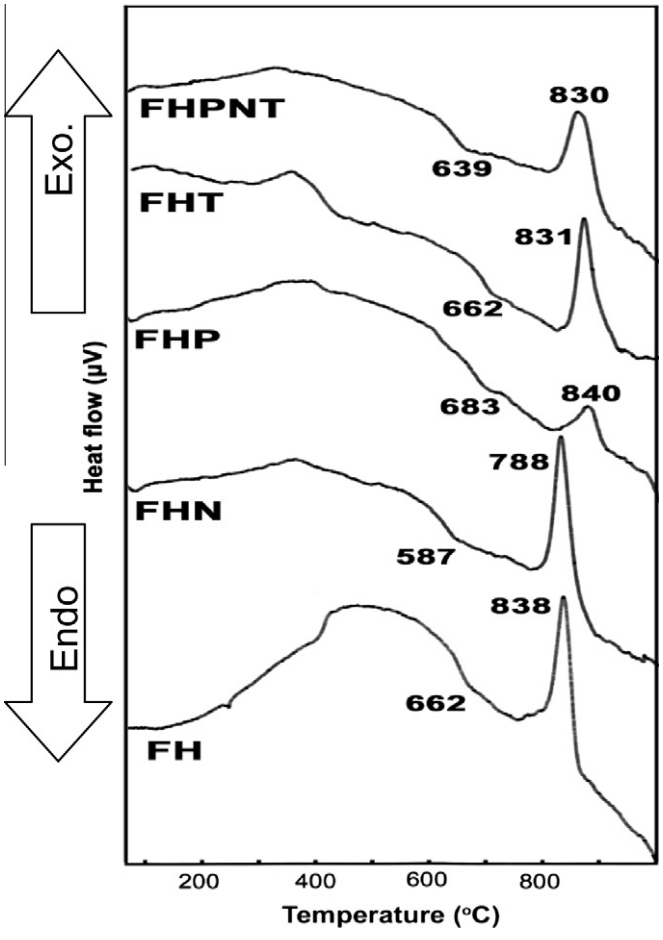

Fig. 1 DTA curves of samples under investigation.

the glasses containing iron ions [16,17], this was clearly noticed for FHPNT sample (639 °C).

The X-ray diffraction patterns of the as prepared samples after cooling from the melting temperature are shown in Fig. 2(a). The picture presents the patterns corresponding to the common structure of magnetite (Fe_3O_4). The diffraction lines of the crystallized magnetite are slightly shifted, as compared with the reference data, indicating a slight variation of the lattice constants of magnetite.

By comparing the XRD pattern of the base sample [4] with those obtained for the samples, after the addition of P_2O_5, Na_2O and TiO_2 (Fig. 2 and Table 3), we could notice that, in general, the amounts of magnetite that crystallizes directly by cooling down the samples from melting temperature were slightly smaller than those precipitated in base glass FH. Adding P_2O_5 (FHP) revealed the crystallization of large amounts of only magnetite phase (slightly lower than base composition). Significant decreases in the amounts of magnetite were detected by adding TiO_2 and Na_2O, respectively. Addition of mixtures of P_2O_5, Na_2O and TiO_2 led to the crystallization of a larger amount of magnetite than that precipitated in FHN and FHT; but still lower than that precipitated in FHP. Traces of hematite appeared in quenched FHPNT samples. It could be clearly seen that all glass–ceramic samples have a high degree of crystallinity, as revealed by sharp peaks. The broadness of the peaks were in the order of FHT > FHN > FHPNT > FHP and consequently the crystallite size was increased in the order of FHT < FHN < FHPNT < FHP (Table 4). The difference in the relative amount of crystallized magnetite in the samples (in spite of that all samples contained the same amount of iron oxide) could be attributed to the different effects of the added oxides on viscosity, phase separation, and the formation of solid solution with magnetite and consequently some iron oxides remain entrapped in the matrix [18].

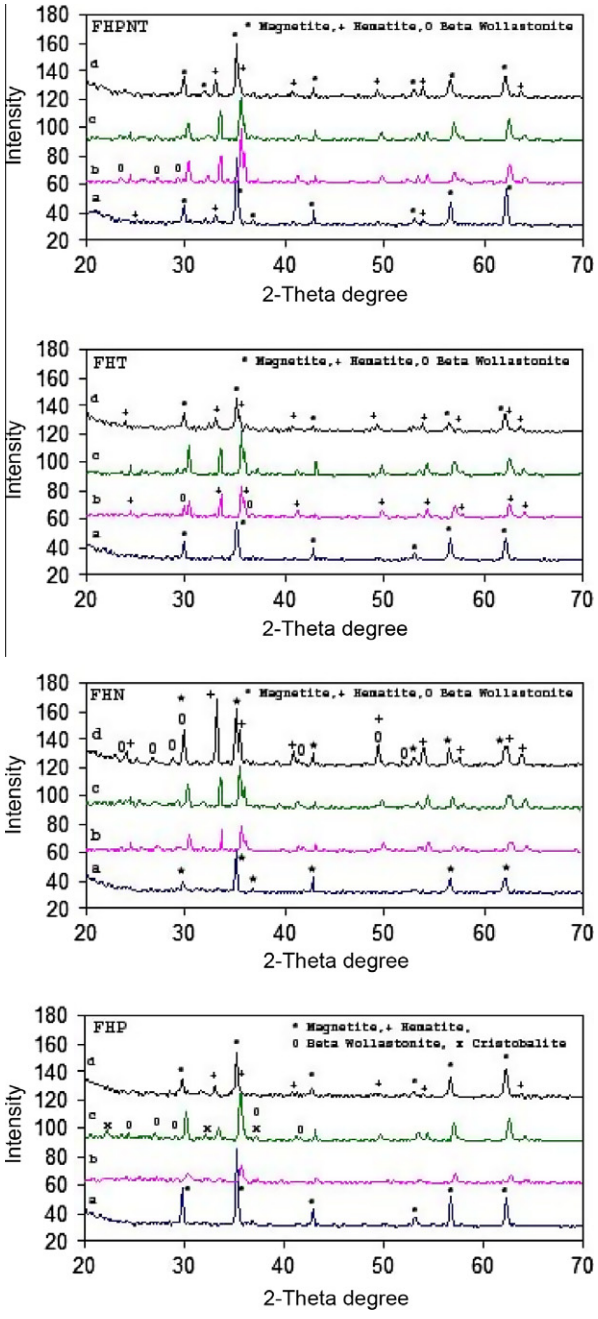

Fig. 2 XRD analysis of FHP, FHN, FHT and FHPNT samples, (a) without heat treatment, (b) heat treated at 1000 °C/1 h, (c) heat treated at 1050 °C/1 h and heat treated at 1050 °C/3 h.

Table 3 Crystallized phases at different heat treatment schedules.

Sample	Heat treatment parameters	Crystallized phases
FHP	As quenched	Magnetite
	1000 °C/1 h	Magnetite, hematite, β-wollastonite
	1050 °C/1 h	Magnetite, hematite, β-wollastonite, cristobalite
	1050 °C/3 h	Magnetite, hematite
FHT	As quenched	Magnetite
	1000 °C/1 h	Magnetite, hematite, β-wollastonite
	1050 °C/1 h	Magnetite, hematite, β-wollastonite
	1050 °C/3 h	Magnetite, hematite
FHN	As quenched	Magnetite
	1000 °C/1 h	Magnetite, hematite, β-wollastonite
	1050 °C/1 h	Magnetite, hematite, β-wollastonite
	1050 °C/3 h	Magnetite, hematite, β-wollastonite
FHPNT	As quenched	Magnetite, hematite
	1000 °C/1 h	Magnetite, hematite, β-wollastonite
	1050 °C/1 h	Magnetite, hematite, β-wollastonite
	1050 °C/3 h	Magnetite, hematite, β-wollastonite

Heat treatments of the samples at different temperatures revealed the crystallization of hematite, and β-wollastonite as minor phases, beside the main crystallized phase of magnetite. Traces of cristobalite appear in FHP sample that was heat treated at 1050 °C/1 h. The amounts of minor crystallized phases depended on the chemical composition and heat treatment schedules. The relative crystallization of hematite and β-wollastonite, with respect to magnetite, was very small

Table 4 Crystallite size of magnetite (nm) for different samples.

Sample	FHN	FHT	FHP	FHPNT
As quenched	71.86	67	90	79.3
1000 °C/1 h	69.5	87.8	54	70.5
1050 °C/3 h	69	60.16	56.37	52

in sample FHP after it was subjected to different heat treatment schedules, while, those phases were largely developed in samples FHPNT, FHT and FHN, respectively (Fig. 2).

Crystallite size obtained from XRD (Fig. 3a and Table 4) showed, in general, the crystallization of nanocrystals of magnetite (< 100 nm). The crystallite size of magnetite in the as quenched samples is relatively increased by adding P_2O_5 and decreased by adding TiO_2. By applying heat treatments, the crystallite size was noticed to decrease greatly in the FHP and FHPNT, while it slightly decreased in the FHT and FHN.

The lattice constants of magnetite (Fig. 3b) revealed an increase in the lattice constants of all the prepared samples than that sited in JCPDS (Joint Committee on Powder Diffraction Standards) cards (a_0 = 8.393–8.399 Å). The effect of different additions on the lattice constants were found to increase in the order of $TiO_2 < P_2O_5 < Na_2O$. The lattice strain had an opposite direction to lattice constants, so the lattice strain was increased in the order of $TiO_2 > P_2O_5$. Increasing the lattice strain led to an increase in the internal forces/stresses which could oppose the crystal growth of magnetite. Consequently, the crystallite size of magnetite, in the case of FHT sample, was slightly lower than that in FHP. By applying heat treatment at different temperatures, the lattice constants were found to increase. Increasing the lattice constant than that cited in JCPDS could be attributed to the incorporation of different cations in a solid solution with magnetite. EDXA (Fig. 4 and Table 5) showed the incorporation of Zn, Ca, and Si in a solid solution with magnetite. It was noticed that the atomic ratio of the incorporated Zn ions in magnetite is quite constant ~5.2Fe:1Zn, mapping of atoms (Fig. 4) detected the presence of Zn atoms adhering to Fe atoms.

TEM of different samples are shown in Fig. 5. The crystallization of one or different phases was evident in TEM micrographs. TEM revealed the precipitation of nanosize rounded crystals of magnetite in the quenched FHP. The crystallite size was decreased by the heat treatment at 1050 °C/3 h, as seen before from XRD analysis. The heat treated FHT showed uniform crystallization of needle like crystals of magnetite. Quenched FHN showed the precipitation of different crystallite shapes of relatively larger sizes, which were dispersed between the small magnetite crystals and coagulation of hay like crystals of hematite appeared, while the heat treated sample revealed uniform crystallization of nanosize crystals. FHPNT heat treated at 1050 °C/3 h revealed uniform distribution of unique rounded nanocrystals of magnetite.

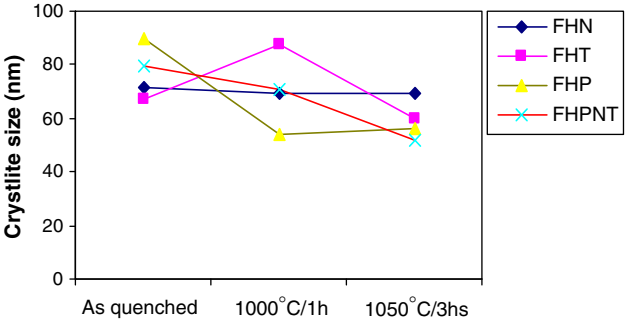

Fig. 3a Crystallite size of different samples at different heat treatment schedules.

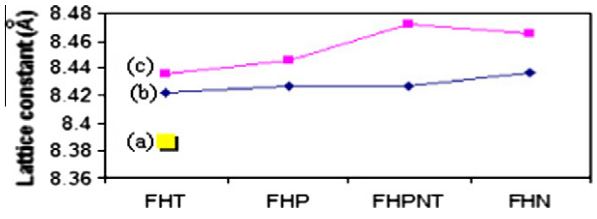

Fig. 3b Variation of lattice constant of magnetite nanocrystals with composition and heat treatment, (a) lattice constant of magnetite from JCPDS cards, (b) lattice constant of magnetite in quenched glass and (c) in glass heat treated at 1050 °C/1 h.

Effects of different additions on the specific magnetization (M_s), remanence (M_r) and coercivity (H_c) of the prepared samples were measured at room temperature in a maximum field of 10 kOe and are summarized in Table 6, while the hysteresis measurements are shown in Fig. 6. It could be observed that all the samples exhibited a similar magnetic behavior, which is characteristic for soft magnetic materials, with a thin hysteresis cycle and low coercive field (< 24 Oe for quenched samples and < 74 Oe for heat treated samples). Magnetic properties were strongly dependent on the added oxides. Saturation magnetization was increased by adding TiO_2 (56.49 emu/g), and P_2O_5 (58.99 emu/g), while being decreased by adding Na_2O in the quenched samples. Addition of mixtures of oxides in FHPNT also revealed a high saturation magnetization ~56.7 emu/g. The coercive field was decreased from 24.76 for FHP and 22.1 for FHT to 19.75 Oe for FHPNT.

Bretcanu et al. [2] measured the saturation magnetization of magnetite particles around 74 emu/g, and the coercive force was 150 Oe, which was lower than the reported data due to the powder form of the sample. They explained this behavior as follows, as the surface/volume ratio was increased, the saturation magnetization was decreased. They calculated the amount of crystallized magnetite from the linear relationship between the saturation magnetization and the content of the magnetite. Therefore, the quantity of magnetite crystallized in the glass–ceramics could be calculated from the ratio of saturation magnetization between the samples and magnetite. The estimated amounts of magnetite crystallized (Table 6) were ~80 wt.% in the FHP, ~76% in FHT and ~77% in FHPNT. Those values are in agreement with the ones estimated by the XRD data. Those values are much higher than the amount of iron oxide added ~60%. This could be attributed to the incorporation of the different cations in magnetite as solid solution. The difference in the amount of magnetite crystallized was matched with the effect of the addition of different oxides in the enhancement of the crystallization of magnetite as cited before. Magnetization increased with the amount of magnetite crystallized in the samples. Glass–ceramic containing higher quantity of magnetite revealed a higher value of saturation magnetization.

The remanence detected is the amount of magnetic materials which could be magnetized, even in the absence of external magnetic field. The remanence magnetization values were much lower than the saturation magnetization values. This could be due to structural features of glass–ceramic [2]. The coercive field depends on the microstructure. In general, as the particle size was increased, the coercive field was decreased.

Heat treatment at 1050 °C/3 h led to a significant decrease in the saturation magnetization (~1, 16 and 44 emu/g for FHN, FHT and FHP, respectively) and to an increase in the

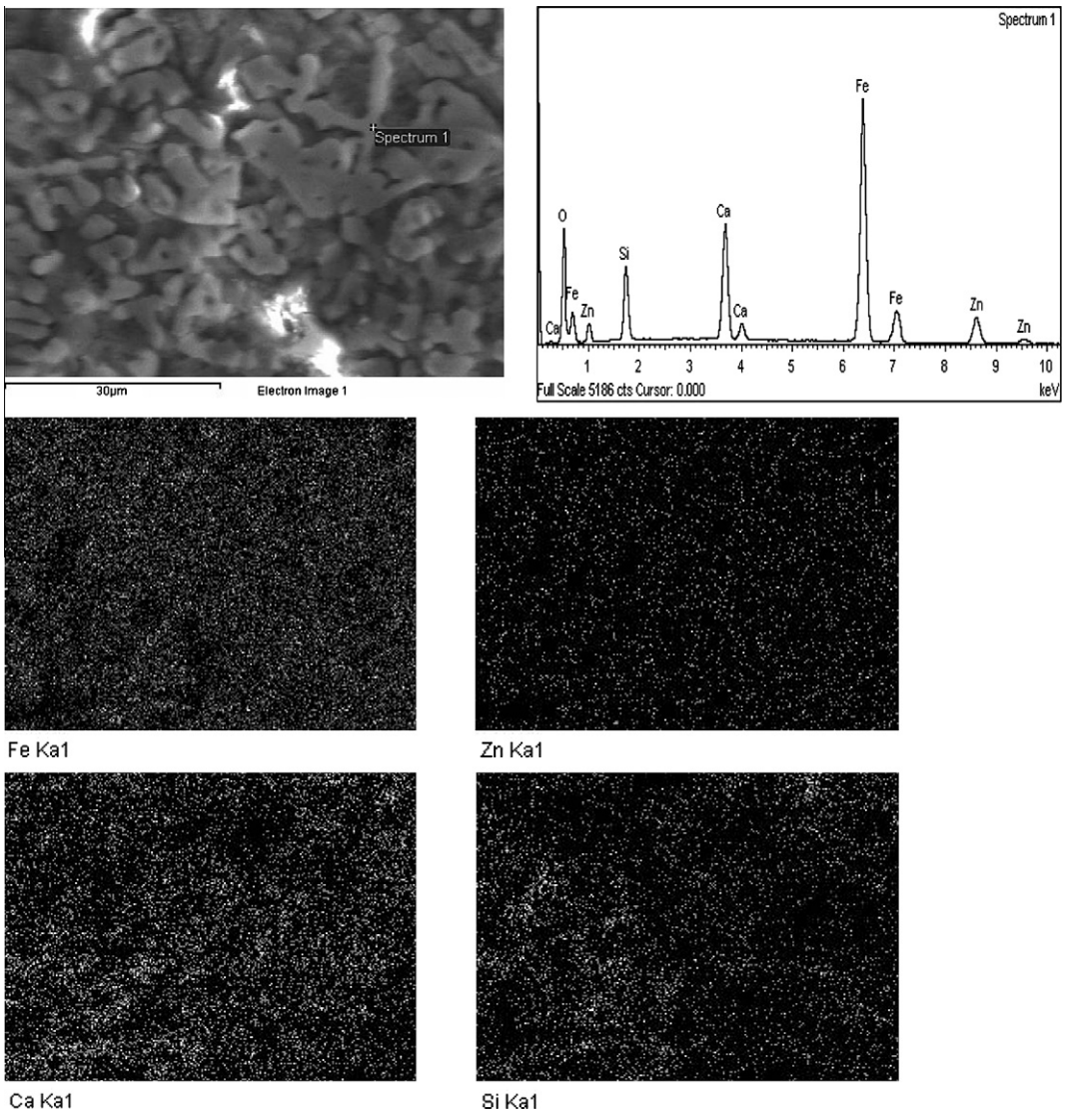

Fig. 4 EDAX of FH sample heat treated at 1000 °C/1 h with mapping pictures.

Table 5 The atomic and weight % of different elements in FH sample heat treated at 1000 °C/1 h by EDAX technique.

Element	Weight %	Atomic %
O K	39.42	66.33
Si K	7.20	6.90
Ca K	8.54	5.73
Fe K	36.61	17.65
Zn K	8.23	3.39
Total	100	100

coercivity (~75, 19 and 22 Oe for FHN, FHT and FHP, respectively) which was attributed to magnetic nanocrystalline anisotropy.

Role of P_2O_5

It has been reported that P_2O_5 increases the nucleation density, which restricts the crystal growth, and induces an amorphous phase separation [18]. P_2O_5 could induce the phase separation to promote a heterogeneous nucleation and then produce a fine-grained interlocking morphology. The heterogeneous nucleation was favorable to reduce the nucleation energy.

The addition of P_2O_5, greatly affects phase formation and morphology. It led to a slight increase in the peak crystallization temperature observed in DTA curves due to the reduction in the number of remaining sites available for magnetite crystallization, where most of the magnetite was crystallized from melt during cooling to room temperature.

Weinberg and co-workers [19] suggested that the nucleation agents could be selectively enriched in one separated phase, thus providing the cites for nucleus. Ryerson [20] proposed that when a modifier cation was added in a silica melt, it was surrounded by both bridging oxygen (O_b) and non bridging oxygen atoms (O_{nb}). The O_{nb} isolates the network-modifier cations from each other by providing screens that mask their positive charge. However, modifier cations that are partly or wholly coordinated by bridging oxygen are poorly shielded from each other. Consequently, substantial columbic repulsions occur between network-modifier cat-

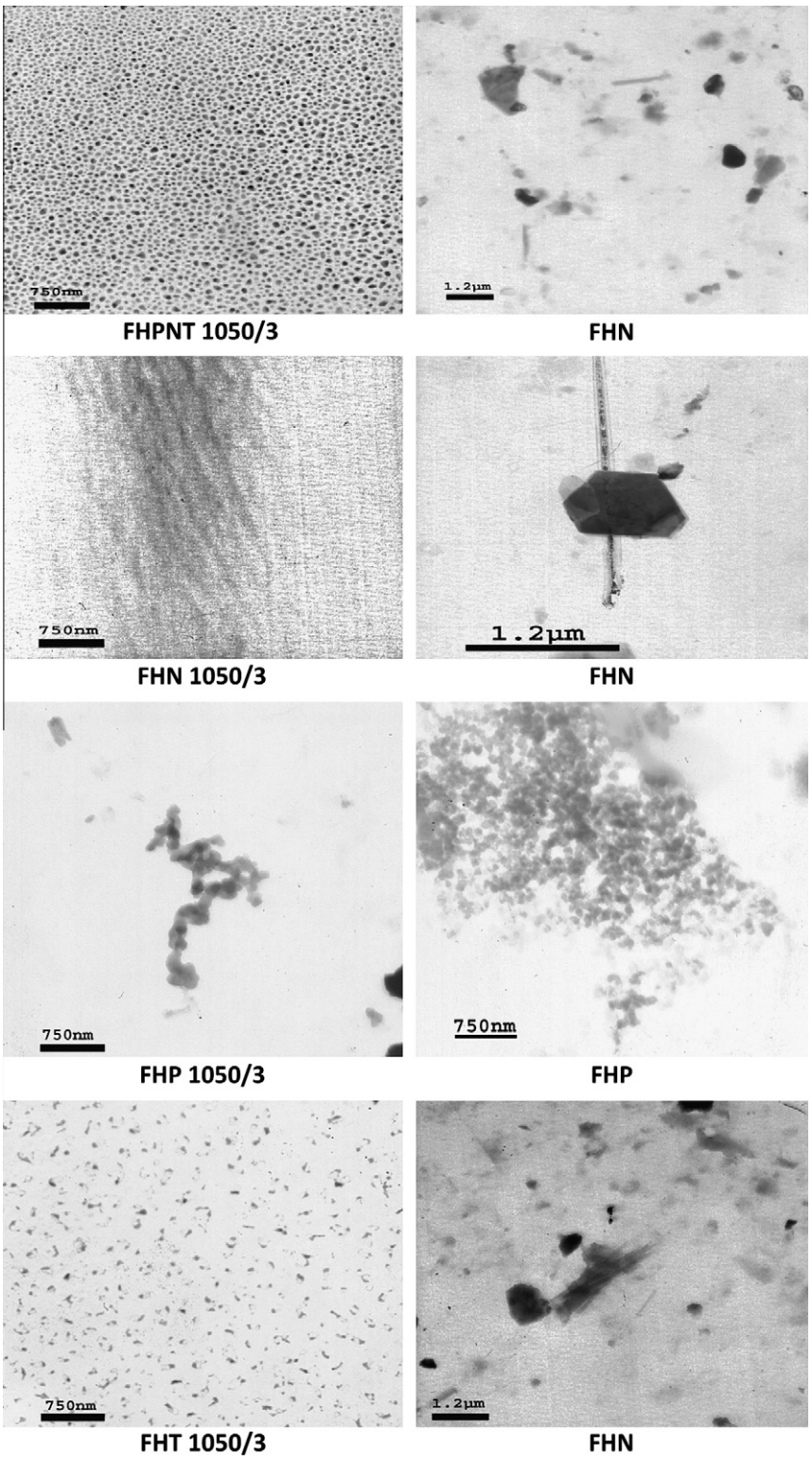

Fig. 5 TEM of different samples after cooling from the melting temperature.

ions which give rise to the enthalpy of unmixing and consequently lead to phase separation [21]. Merzbacher and White found that the immiscibility fields expand with a decrease in the ionic radius of the modifier cation in binary silicate melt [22].

Role of TiO_2

In addition, TiO_2 was reported to induce a phase separation in many compositions [11] by Ti^{4+} ions attracting the non bridged oxygen atoms to the bound arise of bridged domains.

Table 6 Magnetic properties obtained under a maximum magnetic field of 10 kOe.

Sample No.	Heat treatment	Magnetite quantity (wt.%)	Magnetic properties			
			M_s (emu/g)	M_r (emu/g)	M_r/M_s	H_c (Oe)
FHT	Quenched	76	56.49	4.592	0.0812	22.1
FHT	1050 °C/3 h	22	16.01	1.202	0.0750	19.37
FHP	Quenched	80	58.99	4.634	0.0785	24.76
FHP	1050 °C/3 h	60	44.31	3.199	0.0723	22
FHN	1050 °C/3 h	1.39	1.028	0.1864	0.1813	74.85
FHPNT	Quenched	77	56.71	4.129	0.0728	19.75

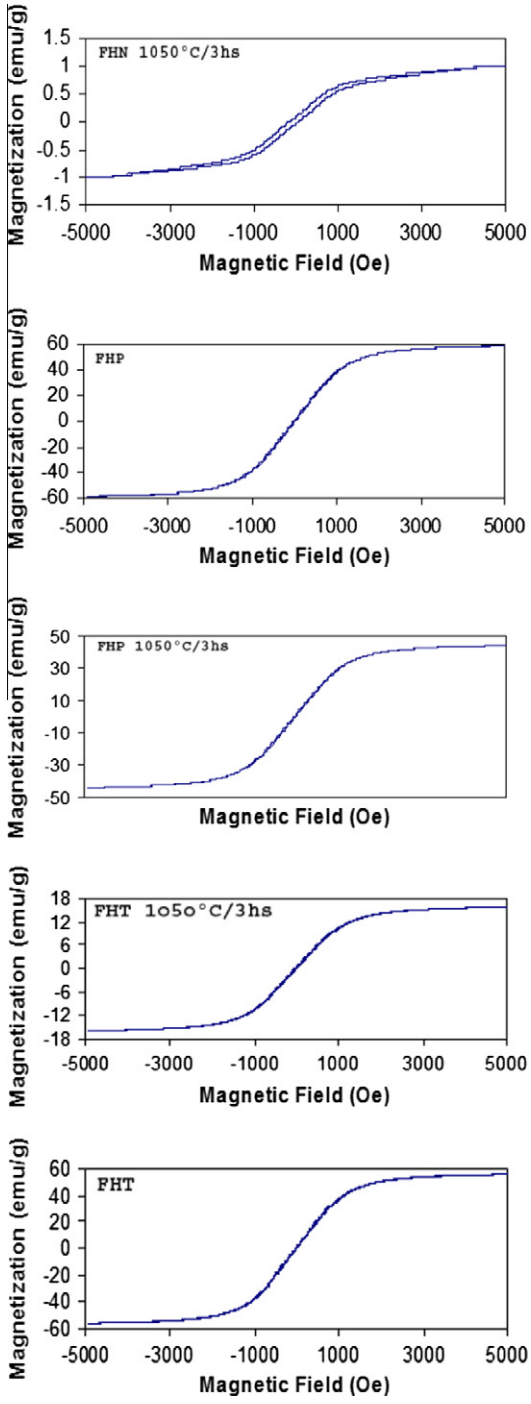

Fig. 6 Effect of different additions and heat treatment on the hysteresis loop.

However, for the formed domains to be stable, each Ti^{4+} must possess no more than two non-bridged oxygen atoms [23]. In the present composition, the number of non-bridged oxygen atoms is far in excess of 2. Thus, it is likely that Ti^{4+} could loosen from the network and crystallize separately in the form of TiO_2 or titanate phases. This would leave P_2O_5 alone to induce the phase separation [24]. This may happen when we mix TiO_2 with P_2O_5 in FHPNT.

It was proposed that, the immiscibility arises, because the melts were composed of network-former as well as network-modifier cations. Those modifier cations compete to form a non-bridging oxygen, in order to properly balance the charge. The greater the possibility for those network-modifiers to be surrounded by a non-bridging oxygen, the greater is the tendency to immiscibility [14].

The incorporation of a small amount of TiO_2 had an influence on the thermal and stability parameters of the phases crystallized at a given heating rate. The temperature difference $T_c - T_g$ was used as an indication of the thermal stability of glasses. The higher the value of this difference, the more the delay in the nucleation process and hence more stable glass was prepared [25].

Role of Na_2O

The crystallization process of the glass during the reheating process was known to be connected with the nature and proportions of its oxide constituents. The ability of some cations to build glass forming units or to be housed as modifiers in interstitial positions in the glass structure should also be considered [26]. Sodium oxide is a good glass modifier and has a beneficial effect in lowering the temperature that is used to convert the glass into a glass–ceramic. It could be housed in the glass structure in the interstices positions which increase the number of non bridging oxygen groups between the (SiO_4) chains, i.e. decrease the stability of the SiO_4 chain [27,28]. This could be attributed to the gradual decrease of viscosity due to the addition of Na^+.

Conclusions

Magnetic glass–ceramic in the system Fe_2O_3·ZnO·CaO·SiO_2 was prepared. The base composition was designed to crystallize about 60% magnetite. The influence of adding TiO_2, Na_2O and P_2O_5 separately or as mixtures was studied. The DTA of the glasses revealed a decrease in the thermal effects by adding P_2O_5, TiO_2 and Na_2O in an increasing order. The X-ray diffraction patterns showed the presence of nanometric magnetite crystals in a glassy matrix after cooling from the melting temperature. The crystallization of magnetite increased by adding TiO_2, P_2O_5, respectively, and decreased by

adding Na_2O. Heat treatment in the temperature range of 1000–1050 °C for different time periods led to the appearance of hematite and β-wollastonite which was slightly increased by adding P_2O_5 or TiO_2 and greatly enhanced by adding Na_2O. Samples containing mixtures of TiO_2, Na_2O, and P_2O_5 showed a summation of the effects of these oxides. The microstructure was studied using TEM which revealed a crystallite size in the range of 52–90 nm. From the obtained hysteresis loops, the saturation magnetization (M_s), remanence magnetization (M_r) and coercivity (H_c) were determined. The results showed that these materials are expected to be useful for localized treatment of cancer.

Acknowledgment

This project was supported financially by the Science and Technology Development Fund (STDF), Egypt, Grant No. 1044.

References

[1] Tartaj P, Del Puerto Morales M, Veintemillas Verdaguer S, González Carreño T, Serna CJ. The preparation of magnetic nanoparticles for applications in biomedicine. J Phys D: Appl Phys 2003;36(13):R182–97.
[2] Bretcanu O, Spriano S, Verné E, Cöisson M, Tiberto P, Allia P. The influence of crystallised Fe_3O_4 on the magnetic properties of coprecipitation-derived ferrimagnetic glass–ceramics. Acta Biomater. 2005;1(4):421–9.
[3] Bretcanu O, Verné E, Cöisson M, Tiberto P, Allia P. Temperature effect on the magnetic properties of the coprecipitation derived ferrimagnetic glass–ceramics. J Magn Magn Mater 2006;300(2):412–7.
[4] Abdel-Hameed SAM, Hessien MM, Azooz MA. Preparation and characterization of some ferromagnetic glass–ceramics contains high quantity of magnetite. Ceram Int 2009;35(4): 1539–44.
[5] Ebisawa Y, Miyaji F, Kokubo T, Ohura K, Nakamura T. Bioactivity of ferrimagnetic glass–ceramics in the system FeO–Fe_2O_3–CaO–SiO_2. Biomaterials 1997;18(19):1277–84.
[6] Hessien MM, Rashad MM, El-Barawy K, Ibrahim IA. Influence of manganese substitution and annealing temperature on the formation, microstructure and magnetic properties of Mn-Zn ferrites. J Magnet Magnet Mater 2008;320(9):1615–21.
[7] Schadewald U, Halbedel B, Romanus H, Hulsenberg D. New results of the crystallization behavior of hexagonal barium ferrites from a glassy matrix. Mat-wiss Werkstofftech 2006;37(11):941–4.
[8] Alizadeh P, Marghussian VK. Effect of nucleating agents on the crystallization behaviour and microstructure of SiO_2–CaO–MgO (Na_2O) glass–ceramics. J Eur Ceram Soc 2000;20(6):775–82.
[9] Mirsaneh M, Reaney IM, Hatton PV, Bhakta S, James PF. Effect of P_2O_5 on the early stage crystallization of K-fluorrichterite glass–ceramics. J Non-Cryst Solids 2008;354(28):3362–8.
[10] Zheng X, Wen G, Song L, Huang XX. Effects of P_2O_5 and heat treatment on crystallization and microstructure in lithium disilicate glass–ceramics. Acta Mater 2008;56(3):549–58.
[11] Arvind A, Sarkar A, Shrikhande VK, Tyagi AK, Kothiyal GP. The effect of TiO_2 addition on the crystallization and phase formation in lithium aluminum silicate (LAS) glasses nucleated by P_2O_5. J Phys Chem Solids 2008;69(11):2622–7.
[12] Hu AM, Li M, Mao DL. Growth behavior, morphology and properties of lithium aluminosilicate glass–ceramics with different amount of CaO, MgO and TiO_2 additive. Ceram Int 2008;34(6):1393–7.
[13] Rezvani M, Eftekhari Yekta B, Solati Hashjin M, Marghussian VK. Effect of Cr_2O_3, Fe_2O_3, and TiO_2 nucleants on the crystallization behavior of SiO_2–Al_2O_3–CaO–MgO–(R_2O) glass–ceramics. Ceram Int 2005;31(1):75–80.
[14] Mingsheng MA, Wen NI, Yali W, Zhongjie W, Fengmei LIU. The effect of TiO_2 on phase separation and crystallization of glass–ceramics in CaO–MgO–Al_2O_3 –SiO_2 –Na_2O system. J Non-Crystal Solids 2008;354(52–54):5395–401.
[15] Khater GA, Idris MH. Role of TiO_2 and ZrO_2 on the crystallizing phases and microstructure in Li, Ba aluminosilicate glass. Ceram Int 2007;33(2):233–8.
[16] Karamanov A, Pelino M. Crystallization phenomena in iron-rich glasses. J Non-Cryst Solids 2001;281(1–3):139–51.
[17] Arcos D, Del Real RP, Vallet Regí M. Biphasic materials for bone grafting and hyperthermia treatment of cancer. J Biomed Mater Res A 2003;65(1):71–8.
[18] Wen G, Zheng X, Song L. Effects of P_2O_5 and sintering temperature on microstructure and mechanical properties of lithium disilicate glass–ceramics. Acta Mater 2007;55(10): 3583–91.
[19] Weinberg MC, Neilson GF, Uhlmann DR. Homogeneous versus heterogeneous crystal nucleation in $Li_2O{\cdot}2SiO_2$ glass. J Non-Cryst Solids 1984;68(1):115–22.
[20] Ryerson FJ, Hess PC. The role of P_2O_5 in silicate melts. Geochm Cosmechim Acta 1980;44(4):611–24.
[21] Agarwal A, Tomozawa M. Determination of fictive temperature of soda-lime silicate glass. J Am Ceram Soc 1995;78(3):827–9.
[22] Merzbacher CI, White WB. The structure of alkaline earth aluminosilicate glasses as determined by vibrational spectroscopy. J Non-Cryst Solids 1991;130(1):18–34.
[23] Barry TI, Clinton D, Lay LA, Mercer RA, Miller RP. The crystallization of glasses based on eutectic compositions in the system Li_2O–Al_2O_3–SiO_2. Part I: Lithium metasilicate-β-spodumene. J Mater Sci 1969;4(7):596–612.
[24] Barry TI, Clinton D, Lay LA, Mercer RA, Miller RP. The crystallization of glasses based on the eutectic compositions in the system Li_2O–Al_2O_3–SiO_2. Part II: Lithium metasilicate-β-eucrypite. J Mater Sci 1970;5(2):117–26.
[25] Park J, Ozturk A. Effect of TiO_2 addition on the crystallization and tribological properties of MgO–CaO–SiO_2–P_2O_5–F glasses. Thermochim Acta 2008;470(1–2):60–6.
[26] Park YJ, Bary PJ. Determination of the structure of glasses in the manganese borate (MnO–B_2O_3) system using ^{11}B NMR. J Korean Phys Soc 1981;14(1):67–74.
[27] Scholze H. Glass: nature, structure and properties. NY: Springer-Verlag; 1990.
[28] Deer WA, Howie RA, Zussman J. An introduction to the rock forming minerals. Hong Kong: Third ELBS impression, Common Wealth, Printing Press Ltd.; 1992.